Recent sedimentation in three adjacent fjord-lakes on the Québec North Shore (Eastern Canada): facies analysis, laminae preservation and potential for varve formation

Obinna P. Nzekwe, Pierre Francus, Guillaume St-Onge, Patrick Lajeunesse, David Fortin, Antoine G. Poiré, Édouard G. H. Philippe, Alexandre Normandeau

O. P. Nzekwe[1] and P. Francus. Institut National de la Recherche Scientifique, Centre - Eau Terre Environnement, Québec, QC G1K 9A9, Canada, Canada Research Chair in Environmental Sedimentology & GEOTOP

Email: obinna_peter.nzekwe@ete.inrs.ca

Email: pierre.francus@ete.inrs.ca

G. St-Onge. Institut des sciences de la mer de Rimouski (ISMER), Université du Québec à Rimouski, QC G5L 2Z9, Canada, Canada Research Chair in Marine Geology & GEOTOP

Email: Guillaume_St-Onge@uqar.ca

P. Lajeunesse and A. G. Poiré. Centre d'études nordiques, Département de géographie, Université Laval, Québec, G1V 0A6, Canada

Email: patrick.lajeunesse@ggr.ulaval.ca

Email: antoine.gagnon-poire.1@ulaval.ca

D. Fortin. School of Earth Sciences and Environmental Sustainability, Northern Arizona University, Flagstaff, AZ 86011, USA

Email: david.fortin@nau.edu

Édouard G. H. Philippe. Institut des sciences de la mer de Rimouski (ISMER), Université du Québec à Rimouski, Canada and Institut de Physique de Globe de Paris, Paris, France & GEOTOP

Email: Edouard.philippe01@gmail.com

A. Normandeau. Geological Survey of Canada (Atlantic), Bedford Institute of Oceanography, Dartmouth, Nova Scotia B2Y 4A2, Canada

Email: alexander.normandeau@canada.ca

[1]Corresponding author. Email: obinna_peter.nzekwe@ete.inrs.ca

Keywords: Limnogeology, sedimentary structures, laminations, varves, CT-scan, Québec North Shore

Submitted to the *Canadian Journal of Earth Sciences*

Abstract

This paper analyzes short gravity cores sampled along transects in three adjacent deep fjord-lakes (lakes Pentecôte, Walker and Pasteur) on the Québec North Shore, Eastern Canada, in order to evaluate the distribution of laminated sediments and potential for varve formation. Facies analysis based on lithological description, digital photos, CT-scan images and bathymetric data allowed for the identification of four main sediment facies, namely: laminated sediments, partially laminated sediments, bioturbated sediments, and massive sediments. Direct evidence that Lake Walker undergoes thermal stratification was monitored from 2014–2016. Mean sedimentation rates and sedimentation fluxes of postglacial sediments in the distal basin of the three studied lakes are ≤ 0.12 cm a^{-1} and 0.03–0.16 g cm^{-2} a^{-1}, respectively based on ^{210}Pb, ^{137}Cs and AMS radiocarbon dating. On the basis of thin section image analysis and ^{210}Pb (CIC) chronology model, Lake Pentecôte contains mainly massive–partially laminated sediments, while Lake Pasteur contains partially laminated sediments and non-annual varve-like sediments. However, Lake Walker contains laminated sediments that are likely varves. The increased potential for laminae preservation observed in Lake Walker compared to lakes Pentecôte and Pasteur is associated with more favourable morphological characteristics including higher relative depth, mean depth, maximum depth and topographic exposure.

Introduction

Lacustrine environments are subject to physical, chemical and biological processes that influence the nature of sediment deposition (Schnurrenberger et al. 2003; Tylmann et al. 2012; Zolitschka et al. 2015). Lake sediments are characterized by sedimentary facies that reflect the processes driving their deposition such as settling, wind-, or density-driven currents (Tylmann et al. 2012). Sedimentary structures such as laminations can be particularly useful for paleoenvironmental reconstructions when they are annually laminated, i.e. formed by seasonal deposition of autochthonous (formed within the lake basin) and/or allochthonous (transported from the watershed to the lake basin) materials under favourable conditions (Larsen and MacDonald 1993; O'Sullivan 1983; Saarnisto 1986; Zolitschka et al. 2015). However, the combination of several environmental and morphological conditions facilitate the preservation of laminations: (1) the absence of sediment-water mixing due to wave or wind-driven circulations, (2) presence of gentle to flat lake bottom that reduces the frequency of mass movements, (3) a deep basin that favours seasonal or permanent axonia, (4) reduced biological activity of benthic organisms, (5) a seasonally contrasted sedimentary supply, and (6) sufficient sedimentation rates (Jenny et al. 2013; Larsen and MacDonald 1993; Larsen et al. 1998; O'Sullivan 1983; Schnurrenberger et al. 2003; Tylmann et al. 2012; Wetzel and Likens 1991; Zolitschka et al. 2015). It has been argued that there is a relationship between the distribution of laminated sediments and the lake morphometry (Zolitschka et al. 2015). Several authors have reported empirical assumptions using morphometric variables in order to improve the chances of recovering laminated sediments during reconnaissance field surveys or in areas where prior studies are relatively limited (e.g. Gorham and Boyce 1989; Larsen and MacDonald 1993; Larsen et al. 1998; O'Sullivan 1983; Ojala et al. 2000; Zolitschka et al. 2015).

On the Québec North Shore, in the southeastern Canadian Shield (Eastern Canada), three lakes (lakes Pentecôte, Walker and Pasteur) were studied for the possible occurrence of annually laminated sediments. High-resolution swath bathymetry, subbottom acoustic profiles and sediment cores were collected to reconstruct the Late Quaternary geomorphological evolution of these fjord-like lakes in response to deglaciation and postglacial sedimentary processes (Gagnon-Poiré 2016; Normandeau et al. 2016). In this paper, short gravity cores retrieved from these three adjacent lakes are analysed in order to evaluate laminae preservation and the potential for varve formation. The specific objectives are to: (1) identify the sedimentary facies present in the short gravity cores and assess their distribution and depositional environments, and (2) evaluate laminae visibility, sedimentation rates and the potential for establishing a varve chronology in the uppermost sediments from the lakes, using radiometric dating (^{210}Pb and ^{137}Cs) and image analysis of thin sections.

Regional setting

Lakes Pentecôte, Walker, and Pasteur are located on the Québec North Shore, in the northwestern Gulf of St. Lawrence in Eastern Canada (Fig. 1). In the local context, the studied lakes are located within the *Reserve faunique de Port-Cartier–Sept-Îles*. They have been fairly undisturbed by anthropogenic activities such as dredging or hydropower generation, except for controlled fishing, boating and wood harvesting. The maximum depths of lakes Pentecôte, Walker and Pasteur are 130, 271 and 70 m, respectively (Gagnon-Poiré 2016); their elevation above sea level (asl) is 84, 115 and 86 m, respectively. The studied lakes have steep sidewalls and relatively deep bottoms, forming a fjord-type morphology. The lakes lie below the limit of the deglacial transgression associated with glacio-isostatic depression, which is at 130 m asl in the region (Dredge 1983).

The Québec North Shore region has a subarctic climate where spring snowmelt, which constitutes the peak of the annual runoff period, occurs usually between April and May. The studied lakes are typically covered by ice from December until April. The lake basins receive seasonal inflows from major rivers and small streams that drain areas covered with glacial fine and marine sediments (Fig. 1). In Lake Walker, the Schmon and Gravel rivers flow into the northwestern and northeastern parts, respectively (Fig. 1). Lakes Pentecôte and Pasteur are principally fed by Pentecôte and Pasteur rivers that both flow into their northern parts (Figs. 1). Land cover is largely a boreal forest comprising fir, black spruce, poplar, aspen and shrubs. Morphological and other characteristics of the lakes are shown in Table 1.

The Québec North Shore region lies within the geologic province of Greenville. Bedrock geology consists of Precambrian rocks that are Archean or Proterozoic in age (Ministère des ressources naturelles du Québec 2002). Archean rocks comprise migmatite and gneiss, which contain plagioclase, biotite and/or hornblende and/or amphibolite. Proterozoic rocks comprise mafic to ultramafic rocks, as well as sedimentary rocks, which contain paragneiss and quartzite (Ministère des ressources naturelles du Québec 2002). Gneissic rocks underlie most parts of lakes Walker and Pentecôte watersheds, while paragneissic rocks underlie most parts of Lake Pasteur. The history of the sedimentation in the watersheds of studied lakes during the transition from late Quaternary glacial to postglacial has been discussed by Gagnon-Poiré (2016), Normandeau et al. (2016) and G. Poiré et al. (accepted). The fjord-type lakes in the southeast Canadian Shield region have been formed by preglacial fluvial erosion during a lower base level, which carved out V-shaped valleys subsequently occupied by Quaternary sediments preserved below the Laurentide Ice Sheet (LIS) (Lajeunesse 2014).

Methods and materials

Fieldwork and sediment coring

Short sediment cores ranging from 30 to 100 cm were collected from lakes Pentecôte, Walker and Pasteur in June 2014. Efforts were made to carefully retrieve undisturbed sediment/water interface from suitable locations based on multibeam bathymetry and subbottom profiler data, which provided insight on the lake basin morphology and nature of sediment deposition. Detailed information on high-resolution subbottom acoustic data from the three studied lakes have been presented by Gagnon-Poiré (2016) and G. Poiré et al. (accepted). Sediment cores were obtained in the central and southern parts of Lake Pentecôte and along two transects in the northern part of Lake Walker (Figs. 2A and 2B). Coring was restricted to the northern part of Lake Pasteur due to limited accessibility (Fig. 2C). A free fall gravity corer (modified after Hvorsley and Stetson 1946) equipped with metal bars as load was used to improve sediment penetration at depths. In total, 42 short gravity cores were collected: 10 cores at Lake Pentecôte, 16 at Lake Walker and 16 at Lake Pasteur (Table 2). The sediment cores were collected on board a pontoon boat on lakes Pentecôte and Walker and from an inflatable boat on Lake Pasteur. All boats were positioned with DGPS systems (*ca* 60 cm precision; Hemisphere GPS, Calgary, Canada).

Temperature sensors (Onset Hobo Water Temp Pro v2 and Tidbit v2 models) were deployed in Lake Walker on June 5th 2014, in order to determine whether the lake undergoes thermal stratification. The deployment location (50°23'17.2" N, 67°10'23.4" W) was chosen for its relative proximity to the area of coring and to the inflow of the two rivers in the northern part of the lake (Fig. 2B). The temperature sensors were placed along a polypropylene rope and set to take readings every hour for a two-year period, after which they were retrieved. To ensure upright suspension of the sensors, a load (concrete block) was tied to the base of the mooring while two buoys located 20 m apart were attached at the upper end of the rope.

On September 25th 2014, during another fieldwork, an S4 current meter (InterOceans Systems Inc. USA) was used to measure temperature and salinity. Two measurements were collected at Lake Pentecôte and three at Lake Walker, at points where the water depths ranged from 40 to 100 m (Table 3). None were collected at Lake Pasteur due to logistical constraints.

Computed tomography and digital photography

Whole core sections were analyzed using a SIEMENS SOMATOM Definition Volume Access sliding gantry medical CT-scanner at the *Institut National de la Recherche Scientifique,* *Centre Eau Terre Environment* (INRS-ETE). The CT-Scan allowed for the non-destructive acquisition of longitudinal and transverse images showing the internal structures of the cores. The acquisition was performed at a voltage of 140 keV, current of 410 mA and a rotation time of 1000 ms/rot. The resulting images were displayed in gray scale, with lighter and darker areas indicating higher and lower X-ray attenuations, respectively. Gray scale values are expressed as CT numbers or Hounsfield units (HU). X-ray attenuation is related to sediment bulk density, porosity and mineralogy (Boespflug et al. 1995; Cremer et al. 2002; Fortin et al. 2013). Analysis of CT-scan images was done using the Siemens software or the Image J software® (Schneider et al. 2012).

Shortly after splitting and prior to oxidation of the sediment core surface, the split sediment cores were photographed with a GEOTEK™ Geoscan IV line-scan camera (50-µm pixel size) mounted on a GEOTEK™ Multi-Sensor Core Logger (MSCL; Geotek Ltd., UK.) at the *Institut des sciences de la mer de Rimouski* (ISMER), Canada. Subsequently, another high-resolution line camera mounted on an ITRAX core scanner (Cox Analytical Systems, Sweden) at INRS-ETE was used to acquire RGB colour images (50-µm pixel size) of the split cores. The advantage of the latter over the former is that the images are relatively free from the effects of glare from water on the sediment surface, due to polarizers of the ITRAX.

Facies- and image analysis

Sediment cores were described and grouped into facies based on qualitative identification of textural properties such as colour, grain size and sedimentary structures through a combination of visual inspections, digital photos, CT-scan images and ITRAX line scan images. Colour of sediments was expressed based on the Munsell Soil Colour Chart (Munsell Color Xrite). A qualitative index, the "Lamination visibility index (LVI)" was introduced to describe the visibility of laminations, as observed from the digital images, with values as follows: 0 - none, 1 - faint, 2 - visible, 3 - clear, and 4 - distinct. One reference core was selected for each lake based on the presence of laminations and evidence of minimal sediment disturbance, namely PC14-04-R (Pentecôte), WA14-06-R (Walker) and PA14-16-R (Pasteur), respectively.

Undisturbed sections were subsampled from the selected reference cores using overlapping metal slabs made of thin aluminium (measuring 18 x 1.5 x 0.5 cm), and thin sections were made based on freeze-drying and epoxy-resin embedding techniques (Francus and Asikainen 2001). Image observation of scanned thin-section slabs was performed using software developed at INRS-ETE (Francus and Nobert 2007). This allowed for further description of the laminae visibility (using the LVI index), and for microscopic counting of laminations on the digital scans (Francus 2006). Laminae were counted by two independent researchers and counting error (%) was estimated based on the difference in the number of counted laminae couplets along the thin sections (Zolitschka et al. 2015).

Sediment dating

For ^{210}Pb analysis, the upper 10 cm section of the three reference cores was sampled at intervals of 0.4 cm. In addition, another core, WA11-W5-R that was retrieved ~2 km southeast of core WA14-06-R during a reconnaissance survey in Lake Walker in 2011, was included in the analysis for comparison (hereafter referred to as reconnaissance core, Fig. 2B). Core WA11-W5-R was previously sampled at intervals of 0.5 cm. Freeze–dried samples (ca. 2g) were analysed for ^{210}Pb activity using a high-resolution germanium diode gamma detector and multichannel analyzer gamma counter at the Centre d'études Nordiques (CEN), Université Laval (Canada) for core WA11-W5-R, and subsequently with a similar instrument at INRS-ETE for the reference cores. ^{210}Pb activities were analysed as function of depth expressed in form of cumulative dry mass in order to account for the effect of compaction (Appleby and Oldfield 1978). The profiles of ^{210}Pb unsupported were used as input for three possible dating models: (1) the constant rate of sedimentation (CRS) model that takes into account variable sedimentation rates, but constant fluxes of ^{210}Pb, (2) the constant initial concentration (CIC) model that simultaneously takes into account varying sedimentation rates and fluxes of ^{210}Pb, and (3) the constant flux - constant sedimentation model (CF-CS) that simultaneously takes into account constant rate of sedimentation and input of ^{210}Pb (Appleby et al. 1979; Robbins and Edgington 1975). Confidence intervals were calculated by first-order error analysis of counting uncertainty (Appleby and Oldfield 1978; Appleby et al. 1979). This was done in order to determine the age (a), sedimentation rate (cm a^{-1}), and sediment (mass) accumulation rates (g cm^{-2} a^{-1}) for the past ~150 years (Zolitschka et al. 2015). ^{137}Cs was used to identify sediments deposited during the peak of atmospheric nuclear testing between the periods from 1963 to 1964 (Appleby and Oldfield 1978).

Terrestrial plant macrofossils (wood fragments) were collected from core WA14-06-R at a depth of 36.5 cm. Bulk sediment from another core, PC15-04B-P-CD that was sampled from Lake Pentecôte in 2015 was included for comparison (G. Poiré et al. accepted). The samples were prepared at CEN and analysed using accelerator mass spectrometry (AMS) at the Earth System Science Department Keck Carbon Cycle AMS Facility at the University of California at Irvine. The dates were calibrated using the Calib 7.1 software using the INTCAL2013 (Stuiver and Reimer 1993) and are presented with 2 sigma standard deviation (Table 4).

Loss on ignition

Within the intervals sampled for ^{210}Pb dating, sediments were extracted to perform loss-on-ignition (LOI) measurements. Organic matter content was calculated as the difference in weight between sediment dried at 60 °C and the ash produced after ignition at 550 °C for 4 hours. Furthermore, the percentage of calcium carbonate was calculated as the difference in weight between ash produced after ignition at 550 and 1000 °C within a high temperature furnace (Heiri et al. 2001).

Results

Physical limnology

Figure 3A shows a clear evidence of temperature variations measured at 35 and 170 m depths (below water level) over a 2-year period (June 5th 2014 – August 4th 2016) in Lake Walker. In the upper part of the lake (~35 m), temperature varied between 3.4 and ~7.0 °C and fluctuated intermittently to 10.0 °C between June and November. It decreased from 3.4 to 2.0 °C during winter. In the lower part of the lake (~170 m), temperature was ~4 °C between June and November, decreasing to ~3.5 °C during winter. Lake mixing, evidenced by temperature reversals across the two depth intervals, occurred twice each year, in May and November, which correspond to the time of ice breakup and ice formation, respectively.

Figures 3B and 3C shows point measurements of temperature and salinity in lakes Pentecôte and Walker measured in September 2014 (Table 3). In Lake Pentecôte, profiles from the northern (S4_PC_01) and southern (S4_PC_03) parts of the lake show a temperature decrease from ~15–12 °C at the surface and ~12–8 °C at 20 meters, and slight increase in salinity from 1.1–1.3 and 1.8–1.9 PSU. Between 20 and 40 m, the northern profile indicates a temperature trend from ~12–9 °C, and slight increase in salinity from 1.2–1.3 PSU, while the southern one shows that towards ~60 m depth, temperature and salinity steadied at ~8 °C and ~1.4 PSU, respectively.

In Lake Walker, profiles from the southern (S4_WA_01) and northern (S4_WA_03) parts show comparable trends between 0–60 m: temperature decreases from ~14–8°C and salinity increases slightly from 1.2–1.4 PSU. Further down, the three parameters stabilize. However, a profile from the central (S4_WA_02) part of the lake indicates that within 0–30 m, temperature decreases from 11–6 °C, while salinity increases slightly from 1.3–1.5 PSU (Figs. 3C-1 and 2). These data show that thermal stratification occurs in Lake Walker.

Sedimentary facies

The following distinct sedimentary facies were identified based on qualitative analysis:

laminated, partially laminated, bioturbated and massive sediments. Rapidly deposited layers and turbidite deposits were also identified (Figs 2, 4 and 5).

Laminated sediments (LS)

The two basic units that compose the laminated sediment facies are a silty minerogenic material (silty lamina) and a clay and organic rich material (clayey lamina). The silty lamina is grayish brown to dark gray (Munsell colour: 2.5Y 5/2 to 4/2), whereas the clayey lamina is dark gray to very dark gray (Munsell colour: 2.5Y 5/2 to 3/2). LS facies have visible to distinct laminations (LVI index 2–4). The thickness of lamina couplets ranges from 0.2 to 1 cm. Laminations are usually horizontal, although sometimes inclined due to disturbance during deposition or coring and transportation. CT number varies from 1100 to 1500 HU (Fig. 5).

The distribution of the LS facies in the three lakes is shown on Figures 2 and 4. Of the ten short sediment cores collected from Lake Pentecôte, none were laminated along its entire length. In Lake Walker, 81% (13 out of 16) of cores were characterised entirely by the LS facies. These cores were retrieved at water depths ranging from 60 to 270 m, which correspond to the deep central part of the lake basin (Figs. 2B, 4B and 4BB). In Lake Pasteur, 6% (1 out of 16) of cores contained LS facies along the entire core. It was retrieved at a depth of 70 m, which corresponds to the deepest part of the lake's basin (Figs. 2C and 4C).

Partially laminated sediments (PLS)

Partially laminated sediments comprise olive gray silty lamina and dark to very dark olive gray clayey lamina (Munsell colour: 5Y 3/15 and Y 4/2 to 3/2, respectively). They are characterized by similar grain size as the LS facies, but with parallel or inclined laminations that range from faint to clear (LVI index 1–3) at intervals within the same core (Fig. 5). Laminae thickness ranges from 0.4 to 1 cm. Wood fragments are more common in the PLS than in the LS facies. CT number varies from 1200 to 1600 HU.

In Lake Pentecôte, partially laminated sediments characterized 80% (8 out of 10) of collected cores. The cores were retrieved from water depths ranging from 39–130 m, representing the shallow to deep parts of the lake (Figs. 2A and 4A). In Lake Walker, none were partially laminated, while in Lake Pasteur, 94% (15 out of 16) of sediment cores were partially laminated. They were collected at water depths ranging from 28–48 m, representing the shallow to moderately deep parts of the lake (Figs. 2C and 4C).

Bioturbated sediment (BS)

Bioturbated sediments are marked by colour mottling, with variation from light yellowish brown to light olive brown and gray to dark grayish brown silty clay and clay materials (Munsell colour: 10YR 6/4 to 4/1, 2.5Y 6/1 to 5/2). The laminations appear faint to visible (LVI index 1–2) and are parallel to inclined, sometimes disturbed. CT number ranges from 1400 to 1500 HU (Fig. 5B).

The BS facies was encountered in the upper part of two cores from Lake Walker, which were retrieved at depths of 10–30 m that correspond to the proximal and shallow parts of the lake (Figs. 2B and 4B).

Massive sediments (MS)

Massive sediments consist of olive gray and dark gray silty and clayey materials (Munsell colour: 5Y 4/2 to 4/1, respectively). There is no clear evidence of visible laminae pattern though faint laminations (LVI index 0-1) are occasionally present (Fig. 5E). This facies contains organic materials such as wood fragments and deformations due to gas expansion that were more evident after core splitting. The transition between the PLS and MS facies are rather subtle.

Of the three studied lakes, sediment cores that present the MS facies were retrieved only in Lake Pentecôte. In that lake, MS facies characterized two cores (Fig. 2A) and also the lower part of another core, PC14-04-R (Fig. 5A). The cores were sampled at water depths of 39–42 m, which corresponds to the shallow parts of the lake (Fig. 2A).

Rapidly deposited layers (RDLs)

Within the LS and PLS facies, there is evidence of a distinct sub-facies that is characterized by light gray to dark yellowish brown silty and clayey materials (Munsell colour: 2.5Y 7/1 to 4/2, 5.Y 3/1), with clearly visible boundaries (LVI index 2–3) that is marked by an abrupt change in CT number from 1300–1500 HU, compared to the LS/PLS facies (Fig. 5). They are interpreted as rapidly deposited layers (RDLs) (St-Onge et al. 2012). RDLs show a sequence of reverse to normal grading (Fig. 5F) and were encountered in several cores from the three studied lakes, irrespective of coring depth. They range from few mm to >1 cm in thickness and are noticeable on CT-scan images and the ITRAX line scan images, but may be obscure under the naked eye (Figs. 5A and 5C). However, a 5 cm thick RDL is clearly noticeable on one core, PA14-16-R from Lake Pasteur (Fig. 5F).

Turbidites

Another sub-facies, characterized by fine grained (silty clay) materials and coarse grained (sandy) materials and which is non-laminated and normally graded, was observed. Its lower and upper boundaries are marked by sharp contacts with the underlying and overlying LS facies, and are evidenced by abrupt change in CT number from 1300 to 1500 HU (Fig. 5D). It is interpreted as a turbidite deposit (St-Onge et al. 2004). It was encountered only in Lake Walker, on one core, WA14-01-R that was collected at a depth of 216 m (Figs. 4BB and 5D).

Thin section image analysis

Laminae visibility index was used to describe thin sections from the three reference cores, PC14-04-R, WA14-06-R and PA14-16-R, and are plotted on Figure 6. Counting of laminae in cross-polarized light was preferred due to higher birefringence of silty particles relative to the fine clay matrix. Image observation of thin sections from core PC14-04-R, collected from Lake Pentecôte at a depth of ~40 m, indicates that it is characterized by MS facies in the lower section that pass into PLS facies in the upper section. The uppermost part appears disturbed near the sediment/water interface. The laminae are faint (LVI index ≤2) and occurrence is discontinuous (Figs. 6A). Consequently, replicate counting of laminae was not performed and thus no counting errors were estimated for this lake.

On thin sections of core WA14-06-R, collected from Lake Walker at 151 m depth, the laminae visibility index shows that laminations appear visible to distinct laminae (index 3–4) in lower to upper intervals, which facilitated replicate counting, but passes into faint laminations (index 0–1) in the uppermost part of the core near the sediment/water interface (Fig. 6B). Approximately 400 lamina couplets were counted along the 43 cm long core, with varying error estimation within successive thin sections. A plot of error estimation versus depth shows that error limit decreases with increasing depth, ranging from 4% for the lowermost part of the core, where distinct laminae were most evident, to 10% for the topmost (5 cm) sediment interval (Figs. 6B and 7B).

On thin sections of core PA14-16-R, collected from Lake Pasteur at 70 m depth, laminations are visible to clear (LVI index 2–3) in the lower part of the core, which facilitated replicate counting (Figs. 6C and 7C), passing into discontinuous and faint (LVI index 0–1) in the uppermost section near the sediment/water interface. Approximately 560 lamina couplets were counted along the 63 cm core. Error estimation versus depth illustrates that the error limit varies irregularly between 3–54% down core (Fig. 6C). Laminae boundaries are noticeably obscured within RDLs, consequently higher error limits were observed where RDLs occur (e.g. between 15–20 cm on core PA14-16-R, Fig. 6C).

Age-depth models and sedimentation rates

^{210}Pb and ^{137}Cs age models

Figure 8 (A-1, B-1 and C-1) depicts ^{210}Pb activity versus depth profiles for the three reference cores. The mean sedimentation- rates and fluxes derived from the three ^{210}Pb models (CRS, CIC and CF-CS) are comparable (Table 5). The ^{210}Pb CIC model was selected as the most suitable model because (1) it is least susceptible to the low activity levels of ^{210}Pb measured on the reference cores (where $^{210}Pb_{total}$ <0.1 Bq g^{-1} except for the top 2 cm), (2) it takes into account the varying sedimentation rates and fluxes of ^{210}Pb that were observed (Fig. S1), and (3) it shows a near-constant slope profile for the three reference cores (Figs. 8A-1, B-1, and C-1). Moreover, the ^{210}Pb CIC model is in close correspondence with the CRS model in the upper sections of cores PC14-04-R and WA14-06-R; and the mean sedimentation rates averaged from both models are similar (Table 5). On the other hand, the ^{210}Pb CF-CS model was the least suitable, as it was most susceptible to decrease in ^{210}Pb unsupported activity levels towards equilibrium, which is evidenced by the wavy outline and age reversals observed (Figs. 8A-2, B-2 and C-2).

On core PC14-04-R (Lake Pentecôte), mean sedimentation rate of ~0.07 cm a^{-1} and mean sedimentation flux of 0.03 g cm^{-2} a^{-1} were calculated based on the ^{210}Pb CIC model, respectively (Table 5). ^{137}Cs activity starts at 1.8 cm and reaches a peak at 0.6 cm sediment depth (Figs. 8A-1 and A-2).

On core WA14-06-R (Lake Walker), mean sedimentation rate of 0.07 cm a^{-1} and mean sedimentation flux of 0.03 g cm^{-2} a^{-1} were calculated based on the ^{210}Pb CIC chronology model, respectively. ^{137}Cs activity starts at 1.4 cm and reaches a peak at 0.6 cm (Figs. 8B-1 and B-2). These values were compared to results from the reconnaissance core, WA11-W5-R (Fig. S2). On that core, mean sedimentation rate of 0.002 cm a^{-1} and mean sedimentation flux of 0.01 g cm^{-2} a^{-1} were calculated based on the ^{210}Pb CIC model, respectively (Table 5). ^{137}Cs activity starts at 2.3 cm and reaches a peak at ~1.3 cm (Fig. S2). The equilibrium depth of ^{210}Pb unsupported (where values tend to zero) corresponds to ~3.75 cm.

On core PA14-16-R (Lake Pasteur), mean sedimentation rate of ~0.12 cm a^{-1} and mean sedimentation flux of 0.09 g cm^{-2} a^{-1} were calculated based on the ^{210}Pb CIC model, respectively (Table 5). ^{137}Cs activity starts at 2.2 cm and reaches a peak at 1.8 cm (Figs. 8C-1 and C-2).

Radiocarbon age

A wood fragment collected from core WA14-06-R at 36.5 cm dated 980 ± 25 years ^{14}C BP (790-920 cal BP, UCIAMS-161059), which allowed for estimation of a mean sedimentation rate of ~0.04 cm a^{-1} for the entire core (Fig. 5C). Bulk sediment sampled at 101 cm from another core, PC15-04B-P-CD from Lake Pentecôte dated 7240 ± 25 years ^{14}C BP (7996-8156 cal BP, UCIAMS-162978) (G. Poiré et al. accepted), and allowed for estimation of a mean sedimentation rate of ~0.09 cm a^{-1} for the entire core (Table 5).

Comparison of laminae counts to radiometric dating

In order to test the hypothesis that the studied lakes could be annually laminated, laminae counts were compared to the ^{210}Pb and ^{137}Cs chronology models for cores WA14-06-R and PA14-16-R from lakes Walker and Pasteur, respectively. Lake Pentecôte was excluded due to low laminae visibility index (index ≤ 2) irrespective of depth.

In Lake Walker, Figure 8B-3 illustrates that the profile of the ^{210}Pb CIC model is consistent with that of laminae couplet counts. Both profiles plots within the error limit (± 6 years) of the other for the uppermost 3 cm sediments interval, and relatively close at lower depths. If the CRS model is considered, there is still close correspondence between the ^{210}Pb CIC versus CRS model and laminae count. The error margin is, however, larger for the CRS model in the lower (3–5cm) part of the core (Fig. 8B-3). The CF-CS model was excluded in the comparison due its high margin of error.

In Lake Pasteur, there is divergence between the ^{210}Pb CIC model and laminae counts. The ^{210}Pb CRS and CF-CS models were less comparable due to age reversals and divergence that are associated with that core (Fig. 8C-3). Figures 8B-3 and 8C-3 show that there is divergence between the profiles of the ^{137}Cs versus ^{210}Pb chronology (CIC) models and also laminae count.

Discussion

Catchment and local controls over sediment deposition

The recent sedimentation in lakes Pentecôte, Walker and Pasteur is influenced by interacting factors including limnological, climatic, morphological and possibly dynamic processes. These lakes undergo thermal stratification typical of the boreal climate in that region, and this was confirmed by instrumentation in Lake Walker (Fig. 3). The transitions between the lower part of the lakes (containing cooler water) and the upper part (containing warmer water), inferred from measured data (30–40 m in Lake Pentecôte and 50–60 m in Lake Walker; Figs. 3B and 3C) corresponds to the summer thermocline in those lakes (Håkanson and Jansson 2002). Temperature reversals observed in Lake Walker indicate that mixing of the water column occurs twice each year, in May and November (Fig. 3A), which implies that it is dimictic. Circulation in its water column occurs to at least 170 m.

Sediment coring in Lake Pentecôte was fairly extensive compared to lakes Walker and Pasteur due to its accessibility. However, the frequency of partially laminated and massive sediments in Lake Pentecôte could be attributed in part to shallow coring depths (generally < 45 m, Table 2) or the influence of processes that inhibit laminae preservation such as sediment mixing due to wind or current driven circulations across the lake's basin (Larsen and MacDonald 1993; O'Sullivan 1983). In Lake Walker, the uniform distribution of laminated sediments (75%) in the distal part of the river deltas (Figs 2B, 5B and 5BB) suggests that sediment deposition is dominated by low-energy suspension settling (Smith 1978; Smith and Ashley 1985). The occurrence of bioturbated facies in two cores that were retrieved in the proximal part of the lake (< 55 m; Figs. 2B and 4B) indicates that sediment disturbance and/or mixing are restricted to the shallow parts of the lake, near the sediment/water interface. It also implies that current and oxic conditions exists in proximal areas near the lake shore, possibly allowing bioturbation (O'Sullivan 1983). Similarly, in Lake Pasteur, the only core that contained LS facies (6 %) was in a deep part, while other cores with PLS facies (94 %) were retrieved from shallower depths (Figs. 2C and 4C).

Lakes Pentecôte, Walker and Pasteur are principally fed by the Pentecôte River, the Gravel and Schmon rivers, and the Pasteur River, respectively from the northern part into the lakes' basin. Although Lake Walker receives fluvial input from two major rivers on its northern part, compared to lakes Pentecôte and Pasteur that receive from one, respectively, the sedimentation rates and fluxes in the central part of the three lakes are of the same order of magnitude, considering the ^{210}Pb models (Figs. 2, Table 5). Also, overall composition of the sediment is similar based on bulk density, calcium carbonate and organic matter contents (Fig. S3). Nevertheless, the low mean sedimentation rates in lakes Pentecôte, Walker and Pasteur ($\leq$ 0.12 cm a^{-1}) are similar to those described in other boreal lakes in southern Québec [e.g. Lake aux Sables: 0.08 cm a^{-1}; Lake St-Joseph: 0.07 cm a^{-1}; and Lake Mékinac: 0.18 cm a^{-1} (Trottier et al, submitted)] and other Canadian provinces [e.g. Birchbark Lake: 0.08 cm a^{-1}; Miller Lake 0.11 cm a^{-1} and Whitemouth Lake (0.15 cm a^{-1}) (Turner and Delorme 1996)].

Relating the presence of laminations to lake morphometry using empirical assumptions

Some researchers have applied empirical relationships to predict laminae formation and preservation in small lakes using morphometric parameters (e.g. Gorham and Boyce 1989; Larsen and MacDonald 1993; Larsen et al. 1998; O'Sullivan 1983; Ojala et al. 2000; Zolitschka et al. 2015). However, there are insights from applying some of those empirical parameters in fjord lakes such as Pentecôte, Walker and Pasteur that are of larger areal size and different geographical context (Table 1). For example, a relevant parameter is the relative depth, Z_r (Hutchinson 1957), which was used by O'Sullivan (1983) to illustrate that lakes with stratified water columns might contain laminated sediments, by relating maximum depth (Z_{max}) and lake surface area (A) [where $Zr = 50Z\sqrt{\pi}/\sqrt{A}$]. In this regard, the relative depth of lakes Pentecôte, Walker and Pasteur is « Z_r = 2.7, 3.9 and 1.4 » respectively (Table 1). These values fall within the range of those of some large lakes in Europe and North America with significant maximum depth (Zm > 70), in which laminated sediments have been found [e.g. Lac D'Annecy, Zm = 82 (Dearing 1979); Pääjärvi, Zm = 87 (Ojala et al. 2000); Lillooet lake, Zm = 137 (Desloges and Gilbert 1994; Gilbert 1975) and Zugersee, Zm = 197 (Thompson and Kelts 1974)].

Larsen and MacDonald (1993) demonstrated that small lakes (<3 km^2) with maximum depths deeper than their critical boundary Zm_1, might preserve laminated sediments, while those with maximum depth Zm less than the depth of Zm_1, are likely to contain non-laminated sediments. That assumption is valid in a general sense when applied to lakes Pentecôte, Walker and Pasteur (with surface area of 18.9, 41 and 19.3 km^2 respectively), based on obtained Zm_1 values and facies distribution (Fig. 4; Tables 1 and 2). However, a modified form of Zm_1, the maximum critical boundary (Zm_m) by Larsen et al. (1998) is inapplicable to lakes Pentecôte, Walker and Pasteur because Zm_m is shallower than the depths from which all cores (except two from Pentecôte) were retrieved.

Alternative variables that describe lake basin morphology, for example by considering both size and depth using mean depth of sampled cores, mean- and maximum wind fetch and exposure index (e.g. Tylmann et al. 2013; Wetzel and Likens 1991) were considered to evaluate facies distribution in lakes Pentecôte, Walker and Pasteur. Table 1 shows that Lake Walker has a mean depth (m = 125) that is significantly deeper than lakes Pentecôte and Pasteur (m = 59.5 and 54.7 respectively), though the three lakes have more or less the same exposure index (ratio of surface area to mean depth). Compared to the other two lakes, Lake Walker also has a longer maximum wind- and mean wind fetch (that describe the distance between coring location and lake shore) due to its greater maximum length (~30 km) and surface area (41 km^2), which suggests that it is exposed to stronger winds that would likely have its water column mixed at relatively greater depths (Wetzel and Likens 1991). However, the fact that LS facies were preserved on 75% of cores collected from Lake Walker compared to lakes Pentecôte and Pasteur

(0 and 6% respectively) indicates that the effects of the longer maximum wind and mean wind fetch are likely compensated by the higher mean depth and maximum depth in the former, as opposed to the latter (Wetzel and Likens 1991). Topographic exposure index calculated for Lake Walker (which is twice as much as the next lake, Pasteur, Table 1) is also a factor favouring laminae preservation (Wetzel and Likens 1991). Thus, morphologically, Lake Walker can be distinguished from lakes Pentecôte and Pasteur based on its unique characteristics: higher relative depth, mean depth, maximum depth and topographic exposure (Table 1).

Laminated vs possibly varved sediments in the three deep fjord-lakes

The potential of establishing a varve chronology differs in the three studied lakes based on the laminae counts and ^{210}Pb dating. In Lake Pentecôte, the prevalence of massive to partially laminated sediment facies and absence of distinct laminations on core PC14-04-R suggest low potential for annual rhythmicity. In Lake Pasteur, the occurrence of partially laminated sediments and the divergence between the ^{210}Pb CIC model versus laminae counts of core PA14-16-R indicate that it contains laminated sediments that are non-annual.

In Lake Walker, close agreement between laminae counts and the ^{210}Pb CIC and CRS chronology models of core WA14-06-R support the hypothesis that the sediments are likely varves. The validity of the depth of ^{137}Cs peak (supposedly 1963) from two cores from Lake Walker is, however, questionable. On core WA14-06-R, the mean sedimentation rate is 0.07 cm a^{-1} (from the CIC model) and the time span between 1963 (^{137}Cs peak) and 2013 (anchor year for the laminae count) is ~50 years. Thus, the supposed depth for the ^{137}Cs peak should be ~3.5 cm « 50 a * 0.07 cm a^{-1} = 3.5 cm » rather than the actual depth, 0.6 cm (Fig. 8B-1). On the reconnaissance core, WA11-05-R, retrieved 3 years earlier, the ^{137}Cs peak is at 1.25 cm (Fig. S2), while the supposed depth should be ~0.094 cm « 47 a * ~0.002 cm a^{-1} = 0.094 cm ». In these two cores, the disparity between the supposed and actual depths of ^{137}Cs peak, yet sharp aspect of the ^{137}Cs peak in the profile suggests possible migration of ^{137}Cs in the sediments, which should be interpreted with caution (e.g. Davis et al. 1984; Turner and Delorme 1996). Another hypothesis is that coring operations using a free-fall gravity corer (also called rocket corer) at great depth (>100 m) do somehow wash away the very unconsolidated water/sediment interface, even if a clear water/sediment interface is apparent in the core tubes. Systematic errors in laminae counting and the chronologies presented could have resulted from technical sources such as sediment sampling that are associated with thin-section preparation, subjective counting of very fine laminae and/or artefacts of the dating models applied (Appleby and Oldfield 1978; Turner and Delorme 1996; Zolitschka et al. 2015). The hypothesis of the laminations in Lake Walker being varves needs to be verified by recovering sediments with other coring techniques, or extensive radiocarbon dating down core where laminae are better preserved, or sediment trap studies (initial deployment of two sediment traps in Lake Walker was unsuccessful). Nevertheless, this study showed that by comparing several ^{210}Pb (CIC, CRS and CF-CS) and ^{137}Cs models, with laminae counts that varves are likely preserved in the upper part of the sedimentary sequence in Lake Walker.

Summary and conclusions

This paper analysed short sediment cores collected across transects alongside subbottom profiles in three deep fjord-lakes (lakes Pentecôte, Walker, Pasteur) on the Québec North Shore, Eastern Canada. The main results are as follows:

- Based on visual description of textural properties supported by CT-scan images and ITRAX line scan images, the following postglacial sedimentary facies were identified: Laminated sediments (LS), Partially laminated sediments (PLS), Bioturbated sediments (BS), and Massive sediments (MS). Rapidly deposited layers (RDLs) and a turbidite deposit were also identified. These facies were deposited under modern conditions, and reflect the influence of interacting factors including seasonality, sedimentation rate and depth.

- Morphological parameters, including relative depth, maximum depth and some variables (mean depth, mean wind fetch, maximum wind fetch and topographic exposure) favour laminae preservation in Lake Walker compared to lakes Pentecôte and Pasteur.
- Lake Pentecôte contains mainly massive to partially laminated sediments, while Lake Pasteur contains (partially) laminated facies that reflect non-annual deposition. On the other hand, Lake Walker contains laminated sediments that are better preserved with increasing depth. Despite inconsistencies in ^{137}Cs dating, there is evidence of close correspondence between laminae counts and the ^{210}Pb (CIC and CRS) chronology models, which support the hypothesis that Lake Walker is likely a varved lake. Therefore, Lake Walker is a promising archive for future varve-based paleoenvironmental reconstructions.

Acknowledgement

The authors thank the Editor, Ali Polat and two anonymous reviewers for constructive reviews in improving this paper. This research was funded by the Natural Sciences and Engineering Research Council of Canada (NSERC) Discovery grants and Ship Time grant, and by the Fonds de Recherche du Québec: Nature et Technologies (FRQNT) – recherche en équipe to P.F, G.S and P.L. Graduate scholarships from GEOTOP (2015) and NSERC CREATE EnviroNorth (2016) to O.N are acknowledged. Reinhard Pienitz at Université Laval is acknowledged for comments and literature that inspired some ideas in this paper. The authors thank members of their research teams: Jean-Philippe Jenny, Arnaud De Coninck, François Lapointe and Thibault Labarrre at INRS-ETE; Etienne Brouard, Annie-Pier Trottier, Francois-Xavier L'Heureux-Houde, Gabriel Joyal and Daniel Deschênes at Université Laval, and Quentin Beauvais, Elissa Barris and Melissa Éttorre at UQAR-ISMER for their assistance during fieldwork and/or in the laboratory. Lastly, we thank the management and staff at *La Réserve faunique de Port-Cartier-Sept-Îles* for ease of access to the lakes.

References

Appleby, P., and Oldfield, F. 1978. The calculation of lead-210 dates assuming a constant rate of supply of unsupported 210 Pb to the sediment. Catena **5**(1): 1-8.

Appleby, P.G., Oldfield, F., Thompson, R., Huttunen, P., and Tolonen, K. 1979. Pb-210 Dating of Annually Laminated Lake-Sediments from Finland. Nature **280**(5717): 53-55.

Boespflug, X., Long, B.F.N., and Occhietti, S. 1995. Cat-Scan in Marine Stratigraphy - a Quantitative Approach. Mar Geol **122**(4): 281-301.

Cremer, J.F., Long, B., Desrosiers, G., de Montety, L., and Locat, J. 2002. Application of scanography to sediment density analysis and sediment structure characterization: Case of sediments deposited in the Saguenay River (Quebec, Canada) after the July 1996 flood. Can Geotech J **39**(2): 440-450.

Davis, R.B., Hess, C.T., Norton, S.A., Hanson, D.W., Hoagland, K.D., and Anderson, D.S. 1984. 137Cs and 210Pb dating of sediments from soft-water lakes in New England (U.S.A.) and Scandinavia, a failure of 137Cs dating. Chem Geol **44**(1): 151-185.

Dearing, J.A. 1979. Application of Magnetic Measurements to Studies of Particulate Flux in Lake-watershed Ecosystems. Ph.D. Thesis, University of Liverpool, U.K.

Desloges, J.R., and Gilbert, R. 1994. Sediment source and hydroclimatic inferences from glacial lake sediments: the postglacial sedimentary record of Lillooet Lake, British Columbia. J Hydrol **159**(1-4): 375-393.

Dredge, L.A. 1983. Surficial geology of the Sept-Îles area, Quebec north shore. Geological Survey of Canada, Vol. 408, Ottawa.

Fortin, D., Francus, P., Gebhardt, A.C., Hahn, A., Kliem, P., Lise-Pronovost, A., Roychowdhury, R., Labrie, J., St-Onge, G., and Team, P.S. 2013. Destructive and non-destructive density determination: method comparison and evaluation from the Laguna Potrok Aike sedimentary record. Quaternary Sci Rev **71**: 147-153.

Francus, P. (ed). 2006. Image Analysis, Sediments and Paleoenvironments. Developments in Paleoenvironmental Research, vol. 7. Springer, Dordrecht.

Francus, P., and Asikainen, C.A. 2001. Sub-sampling unconsolidated sediments: A solution for the preparation of undisturbed thin-sections from clay-rich sediments. Journal of Paleolimnology **26**(3): 323-326.

Francus, P., and Nobert, P. 2007. An integrated computer system to acquire, process, measure and store images of laminated sediments. *In* 4th International Limnogeology Congress, Barcelona, Spain (11–14th July).

Gagnon-Poiré, A. 2016. Sédimention tardi-quaternaire glaciaire à postglaciaire dans trois fjords lacustres adjacents du sud-est du Bouclier canadien. *In* (Mémoire de maîtrise non publiée) Centre d'études nordiques, Département de géographie. Université Laval, Québec.

Gilbert, R. 1975. Sedimentation in Lillooet Lake, British Columbia. Can J Earth Sci **12**(10): 1697-1711.

Gorham, E., and Boyce, F.M. 1989. Influence of lake surface area and depth upon thermal stratification and the depth of the summer thermocline. J. Great Lakes Res. **15**(2): 233-245.

Håkanson, L., and Jansson, M. 2002. Principles of Lake Sedimentology, 2nd ed. The Blackburn Press, New Jersey. pp. 316.

Heiri, O., Lotter, A.F., and Lemcke, G. 2001. Loss on ignition as a method for estimating organic and carbonate content in sediments: reproducibility and comparability of results. Journal of paleolimnology **25**(1): 101-110.

Hutchinson, G. 1957. A treatise on limnology. Vol. 1. Geography, physics, and chemistry. John Wiley&Sons. Inc. New York: 1015.

Hvorsley, M.J., and Stetson, H.C. 1946. Gravity coring instruments and mechanics of sediment coring. Bull. Geol. Soc. **57**: 935.

Jenny, J.-P., Arnaud, F., Dorioz, J.-M., Giguet Covex, C., Frossard, V., Sabatier, P., Millet, L., Reyss, J.-L., Tachikawa, K., and Bard, E. 2013. A spatiotemporal investigation of varved sediments highlights the dynamics of hypolimnetic hypoxia in a large hard-water lake over the last 150 years. Limnol Oceanogr **58**(4): 1395-1408.

Lajeunesse, P. 2014. Buried preglacial fluvial gorges and valleys preserved through Quaternary glaciations beneath the eastern Laurentide Ice Sheet. Geol Soc Am Bull **126**(3-4): 447-458.

Larsen, C.P.S., and MacDonald, G.M. 1993. Lake morphometry, sediment mixing and the selection of sites for fine resolution palaeoecological studies. Quaternary Sci Rev **12**(9): 781-792.

Larsen, C.P.S., Pienitz, R., Smol, J.P., Moser, K.A., Cumming, B.F., Blais, J.M., Macdonald, G.M., and Hall, R.I. 1998. Relations between lake morphometry and the presence of laminated lake sediments: A re-examination of Larsen and Macdonald (1993). Quaternary Sci Rev **17**(8): 711-717.

Ministère des ressources naturelles du Québec. 2002. Carte géologique du Québec. Ministère des ressources naturelles, Québec, DV 2002-06, Québec.

Normandeau, A., Lajeunesse, P., Poiré, A.G., and Francus, P. 2016. Morphological expression of bedforms formed by supercritical sediment density flows on four fjord□lake deltas of the south□eastern Canadian Shield (Eastern Canada). Sedimentology **63**(7): 2106-2129.

O'Sullivan, P.E. 1983. Annually-laminated lake sediments and the study of Quaternary environmental changes — a review. Quaternary Sci Rev **1**(4): 245-313.

Ojala, A.E., Saarinen, T., and Salonen, V.-P. 2000. Preconditions for the formation of annually laminated lake sediments in southern and central Finland. Boreal Environment Research **5**(3): 243-255.

Robbins, J.A., and Edgington, D.N. 1975. Determination of recent sedimentation rates in Lake Michigan using Pb-210 and Cs-137. Geochim Cosmochim Ac **39**(3): 285-304.

Saarnisto, M. 1986. Annually laminated lake sediments. *In* Handbook of Holocene palaeoecology and palaeohydrology. *Edited by* B. B.E. John Wiley and Sons Ltd, Chichester. pp. 343-370.

Schneider, C.A., Rasband, W.S., and Eliceiri, K.W. 2012. NIH Image to ImageJ: 25 years of image analysis. Nature methods **9**(7): 671.

Schnurrenberger, D., Russell, J., and Kelts, K. 2003. Classification of lacustrine sediments based on sedimentary components. Journal of Paleolimnology **29**(2): 141-154.

Smith, N.D. 1978. Sedimentation processes and patterns in a glacier-fed lake with low sediment input. Can J Earth Sci **15**(5): 741-756.

Smith, N.D., and Ashley, G.M. 1985. Proglacial lacustrine environment. *In* Glacial Sedimentary Environments. *Edited by* G.M. Ashley and J. Shaw and J.A. Smith. Soc. Econ. Peleont. Miner., Tulsa, Oklahoma.

St-Onge, G., Chapron, E., Mulsow, S., Salas, M., Viel, M., Debret, M., Foucher, A., Mulder, T., Winiarski, T., and Desmet, M. 2012. Comparison of earthquake-triggered turbidites from the Saguenay (Eastern Canada) and Reloncavi (Chilean margin) Fjords: Implications for paleoseismicity and sedimentology. Sediment Geol **243**: 63-107.

St-Onge, G., Mulder, T., Piper, D.J.W., Hillaire-Marcel, C., and Stoner, J.S. 2004. Earthquake and flood-induced turbidites in the Saguenay Fjord (Quebec): a Holocene paleoseismicity record. Quaternary Sci Rev **23**(3-4): 283-294.

Stuiver, M., and Reimer, P.J. 1993. Extended 14 C data base and revised CALIB 3.0 14 C age calibration program. Radiocarbon **35**(01): 215-230.

Thompson, R., and Kelts, K. 1974. Holocene sediments and magnetic stratigraphy from Lakes Zug and Zurich, Switzerland. Sedimentology **21**(4): 577-596.

Turner, L.J., and Delorme, L.D. 1996. Assessment of 210Pb data from Canadian lakes using the CIC and CRS models. Environmental Geology **28**(2): 78-87.

Tylmann, W., Szpakowska, K., Ohlendorf, C., Woszczyk, M., and Zolitschka, B. 2012. Conditions for deposition of annually laminated sediments in small meromictic lakes: a case study of Lake Suminko (northern Poland). Journal of Paleolimnology **47**(1): 55-70.

Tylmann, W., Zolitschka, B., Enters, D., and Ohlendorf, C. 2013. Laminated lake sediments in northeast Poland: distribution, preconditions for formation and potential for paleoenvironmental investigation. Journal of Paleolimnology **50**(4): 487-503.

Wetzel, R.G., and Likens, G.E. 1991. Limnological Analyses. 2nd Edition ed. Springer-Verlag. pp. 391.

Zolitschka, B., Francus, P., Ojala, A.E.K., and Schimmelmann, A. 2015. Varves in lake sediments – a review. Quaternary Sci Rev **117**(0): 1-41.

List of Tables

List of Figures

Fig. 1. (A) Geographic location of the Québec North Shore region in Eastern Canada. The insert (B) shows the location of lakes Pentecôte (PC), Walker (WA) and Pasteur (PA) (shown in blue background) and the extent of their respective watersheds (marked by dark lines). Major river inflows in the northern area of each lake are also shown.

Fig. 2. Maps showing bathymetry, location of sediment cores and the sediment facies described in (A) Lake Pentecôte, (B) Lake Walker and (C) Lake Pasteur. Core names are abbreviated as serial numbers e.g. WA14-**06**-R written as 6 (Table 1). W5 refers to the reconnaissance core, WA11-**W5**-R from Lake Walker (see text). Also shown is the deployment location of Onset temperature sensors in Lake Walker, labelled as T. Schematic subbottom profiles along marked transects are shown in Fig. 3. Core names along transect c-c', Lake Pasteur, are clearer in Fig. 4D

Fig 3. Measurement of physical parameters: (A) Temperature variations in the water column of Lake Walker at 35 and 170 m depths measured using Onset Hobo temperature sensors over a 2-year period (June 2014 – July 2016). Deployment location of sensors is marked as T in the Fig. 2. (B and C) Profiles of temperature and salinity measured in lakes Pentecôte and Walker, respectively using an S4 current meter on September 24 2014 (sampling points are described in Table 3)

Fig. 4. Schematic subbottom profiles along the transects shown in Fig. 2. (A) a – a', Lake Pentecôte; (B) (b – b', bb – bb', Lake Walker) and (C) c – c', Lake Pasteur. The location of cores retrieved and the sediment facies encountered are shown (see full legend in Fig. 2). Core names are abbreviated as serial numbers (see Table 1). RF indicates the reference core for each lake. Thermal stratification zones are inferred from temperature measurements (see text). Also shown are the empirical depths of the critical boundary (Zm_1) described for each lake (See text and Table 1)

Fig. 5. Digital photo (Ph), ITRAX line scan images (L) and CT-scan frontal view (CT) showing example images of the sedimentary facies described in lakes Pentecôte, Walker and Pasteur. Rapidly deposited layers (RDLs) and turbidites (TB) represent isolated events. The LLS (?) represents proglacial facies that was encountered (below the BS facies, 5B) but not discussed in detail in this study (see core PC15-04-P-CD; G. Poiré et al. accepted). Note that corresponding images may appear slightly different because they were taken along different slices/views of the respective sediment cores

Fig. 6. Profiles with the digital photo (Ph), ITRAX line scan image (L) and CT-scan frontal view (CT), and results of sedimentological analysis: laminae visibility index (LVI) and laminae counting error estimate for the reference cores (A) PC14-04-R, (B) WA14-06-R and (C) PA14-16-R from lakes Pentecôte, Walker and Pasteur, respectively. LVI index: 0 - none, 1- faint, 2 - visible, 3 - clear, 4 - distinct. Thin-sections from the lower part (marked "TS" on the digital photos) are shown in Fig. 7

Fig. 6 (continued, 6C) Profiles with the digital photo, CT-scan frontal view, line scan image (ITRAX) and results of sedimentological analysis: laminae visibility index (LVI) and laminae counting error estimate for the core PA14-16-R from Lake Pasteur. LVI index: 0 - none, 1- faint, 2 - visible, 3 - clear, 4 - distinct. Thin-sections from the lower part (marked "TS" on the digital photos) are shown in Fig. 7

Fig. 7. Image observation of laminae structure in lower intervals of the reference cores: (A) PC14-04-R, (B) WA14-06-R and (C) PA14-16-R using thin-sections viewed in plane (left) and cross polarized light (right). Scale is 1 cm. Blue backgrounds in the cross-polars are due to the embedding resin. In the WA14-06-R and PA14-16-R, visible–distinct laminae couplets comprising a silty lamina and a clayey lamina with sharp contact with the overlying laminae can be seen

Fig. 8. Recent chronology (^{210}Pb and ^{137}Cs) for the reference cores from (A) Lake Pentecôte, (B) Lake Walker and (C) Lake Pasteur, respectively: (A-1, B-1, and C-1) Total (measured) and supported (from ^{226}Ra decay) ^{210}Pb activity and ^{137}CS activity; (A-2, B-2, and C-2) Chronology models based on the constant rate of supply (CRS), the constant initial concentration (CIC) and constant flux–constant sedimentation (CF-CS); (B-3, and C-3) Comparison of applicable age models (CIC/CRS) to lamina couplet counts in the upper sediments of lakes Walker and Pasteur

Table 1. Characteristics of the studied lakes and empirical parameters relating laminated sediments to lake morphometry

Lake	Pentecôte	Walker	Pasteur
Latitude (˚)	49.867	50.267	50.217
Longitude (˚)	-67.333	-67.15	-66.067
Altitude (m)	84	115	86
Maximum depth, Zm (m)	130	271	70
Maximum lenght, L_{max} (km)	15	30	18
Maximum width, b_{max} (km)	2.8	2.3	1.9
Lake area (km^2)	18.9	41	19.3
Area of watershed (km^2)	1710	2173	1020
Salinity (PSU)	1.2 - 1.4	1.2 - 1.5	
Conductivity (mS)	1.75 - 1.9	1.75 - 1.9	
Thermal lake type	D	D	D
Catchment Geology	G, T, S, C, P	G, T, S, C, P	Pg, T, S, C, P
Dominant sediment facies	MS, PLS	LS	PLS
Empirical assumptions			
Relative depth, Z_r (m)	2.7	3.9	1.4
Critical boundary, Zm_1 (m)	71.5	89.8	72.5
Mean depth (m)	59.5	125	54.7
Exposure index (km)	31.8	32	35.3
Maximum wind fetch (km)	5.3	6.1	2.3
Mean wind fetch (km)	1.6	1.9	0.9
Topographic exposure (km)	28.4	125.6	52.2
Shoreline development (%)	5	3	1
Shoreline afforestation (%)	80	85	70

Basic morphometric characteristics according to (Gagnon-Poiré 2016; Normandeau et al. 2016). Thermal lake type: D - dimictic. Catchment geology: G gneiss, Pg paragniess, T morainic till, S sand and gravel, C clay and silt, P peat. Empirical assumptions (Hutchinson 1957; Larsen and MacDonald 1993; Tylmann et al. 2013; Wetzel et al. 1991). Facies legend is given in Table 2.

Table 2. List of sediment cores sampled from the three studied lakes

S/N	Core name	Lake	Latitude (N)	Longitude (W)	Water depth (m)	Length (m)	Main sediment facies (Remark)
1	PC14-01-R	Pentecôte	49.880944	67.356639	43	37	PLS
2	PC14-02-R	Pentecôte	49.882444	67.354611	38	37	PLS
3	PC14-03-R	Pentecôte	49.883556	67.353667	50	35	PLS
4	PC14-04-R	Pentecôte	49.884944	67.353167	40	39	PLS (Reference)
5	PC14-05-R	Pentecôte	49.886306	67.351250	45	39	PLS
6	PC14-06-R	Pentecôte	49.869208	67.331844	80	38	PLS
7	PC14-07-R	Pentecôte	49.858361	67.331056	130	42	MS
8	PC14-08-R	Pentecôte	49.858361	67.318028	90	41	PLS
9	PC14-09-R	Pentecôte	49.837972	67.296222	39	39	PLS
10	PC14-10-R	Pentecôte	49.829611	67.286444	40	40	MS
0	WA14-00-R	Walker	50.394111	67.172389	161	43	LS
1	WA14-01-R	Walker	50.369750	67.167861	216	54	LS
2	WA14-02-R	Walker	50.369083	67.170806	178	55	LS
3	WA14-03-R	Walker	50.368250	67.174694	140	48	LS
4	WA14-04-R	Walker	50.367722	67.177083	121	46	LS
5	WA14-05-R	Walker	50.367361	67.178556	69	44	LS
6	WA14-06-R	Walker	50.380306	67.174028	151	49	LS
7	WA14-07-R	Walker	50.379083	67.176306	140	48	LS (Reference)
8	WA14-08-R	Walker	50.377361	67.177083	140	45	LS
9	WA14-09-R	Walker	50.377083	67.181806	57	40	LS
10	WA14-10-R	Walker	50.376639	67.184139	31	35	BS
11	WA14-11-R	Walker	50.375917	67.185750	11	30	BS
12	WA14-12-R	Walker	50.381417	67.170028	157	44	LS
13	WA14-13-R	Walker	50.382889	67.165361	130	46	LS
14	WA14-14-R	Walker	50.368111	67.172028	165	48	LS
15	WA14-15-R	Walker	50.367917	67.175694	139	43	LS
W5	WA11-W5-R	Walker	50.362310	67.165650	270	43	LS (Reconnaissance)
2	PA14-02-R	Pasteur	50.318667	66.927083	30	38	PLS
3	PA14-03-R	Pasteur	50.318583	66.927361	39	39	PLS
4	PA14-04-R	Pasteur	50.318722	66.927639	46	35	PLS
5	PA14-05-R	Pasteur	50.318778	66.927889	50	41	PLS
6	PA14-06-R	Pasteur	50.318833	66.928222	55	36	PLS
7	PA14-07-R	Pasteur	50.318806	66.928417	59	39	PLS
8	PA14-08-R	Pasteur	50.318806	66.928722	65	42	PLS
9	PA14-09-R	Pasteur	50.318917	66.929083	69	39	PLS
10	PA14-10-R	Pasteur	50.319583	66.934972	38	28	PLS
11	PA14-11-R	Pasteur	50.319175	66.932806	62	38	PLS
12	PA14-12-R	Pasteur	50.319167	66.932528	67	36	PLS
13	PA14-13-R	Pasteur	50.324806	66.933778	45	34	PLS
14	PA14-14-R	Pasteur	50.332333	66.935083	60	40	PLS
15	PA14-15-R	Pasteur	50.334167	66.937056	57	48	PLS
16	PA14-16-R	Pasteur	50.318972	66.929944	71	66	LS (Reference)
17	PA14-17-R	Pasteur	50.318861	66.928694	65	77	PLS

Sediment facies: LS - Laminated sediments, PLS - Partially laminated sediments, BS - Bioturbated sediments, MS - Massive sediments

Table 3. List of sampling points for measurement of physico-chemical parameters in lakes Pentecôte and Walker

Code	Lake	Latitude (N)	Longitude (W)	Parameter measured	Depth (m)	Relative location
S4_PC_01	Pentecôte	49.918368	67.362836	T, S	40	North
S4_PC_03	Pentecôte	49.842510	67.305110	T, S	60	South
S4_WA_01	Walker	50.222500	67.150833	T, S	100	South
S4_WA_02	Walker	50.299067	67.182238	T, S	60	Central
S4_WA_03	Walker	50.377083	67.181806	T, S	80	North
T1 (Onset)	Walker	50.338111	67.173167	T	35	North-central
T12 (Onset)	Walker	50.338111	67.173167	T	170	North-central

Parameter: T- temperature, S – salinity. Measurement points and profiles are shown on Figures 2 and 3, respectively.

Table 4. AMS ^{14}C age of the dated materials from lakes Pentecôte and Walker

Core name	**Depth (cm)**	**Material**	**Laboratory no.**	**^{14}C âge (BP)**	**^{14}C âge calBP**
WA14-06-R	36.5	Wood fragment	UCIAMS-161059	930 ± 25	791-918
PC15-04B-P-CD*	101	Bulk sediment	UCIAMS-162978	7240 ± 25	7996-8159

*G. Poiré et al. (accepted)

Table 5. Comparison of sedimentation- rates and fluxes derived from sediment dating from surface cores from lakes Pentecôte, Walker and Pasteur

Core	**Sedimentation rate (mm a^{-1})***				**Sedimentation flux (g cm^{-2} a^{-1})**		
	^{210}Pb CRS	^{210}Pb CIC	^{210}Pb CF-CS	AMS ^{14}C	^{210}Pb CRS	^{210}Pb CIC	^{210}Pb CF-CS
PC14-04-R	0.64	0.68	0.48		0.03	0.03	0.02
WA14-06-R	0.65	0.70	0.95	0.40	0.03	0.03	0.05
PA14-16-R	0.04	1.15	0.87		0.03	0.09	0.06
WA11-W5-R	0.11	0.02	0.02		0.03	0.01	0.16
PC15-04B-P-CD*				0.90			

*G. Poiré et al. (accepted)

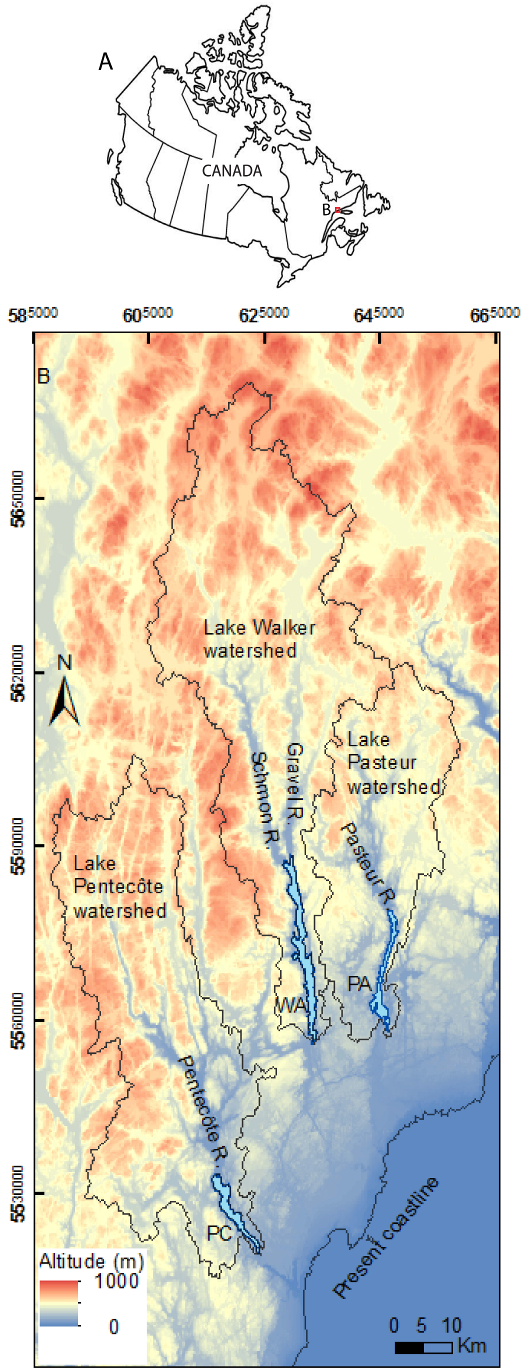

Fig. 1. (A) Geographic location of the Québec North Shore region in Eastern Canada. The insert (B) shows the location of lakes Pentecôte (PC), Walker (WA) and Pasteur (PA) (shown in blue background) and the extent of their respective watersheds (marked by dark lines). Major river inflows in the northern area of each lake are also shown.

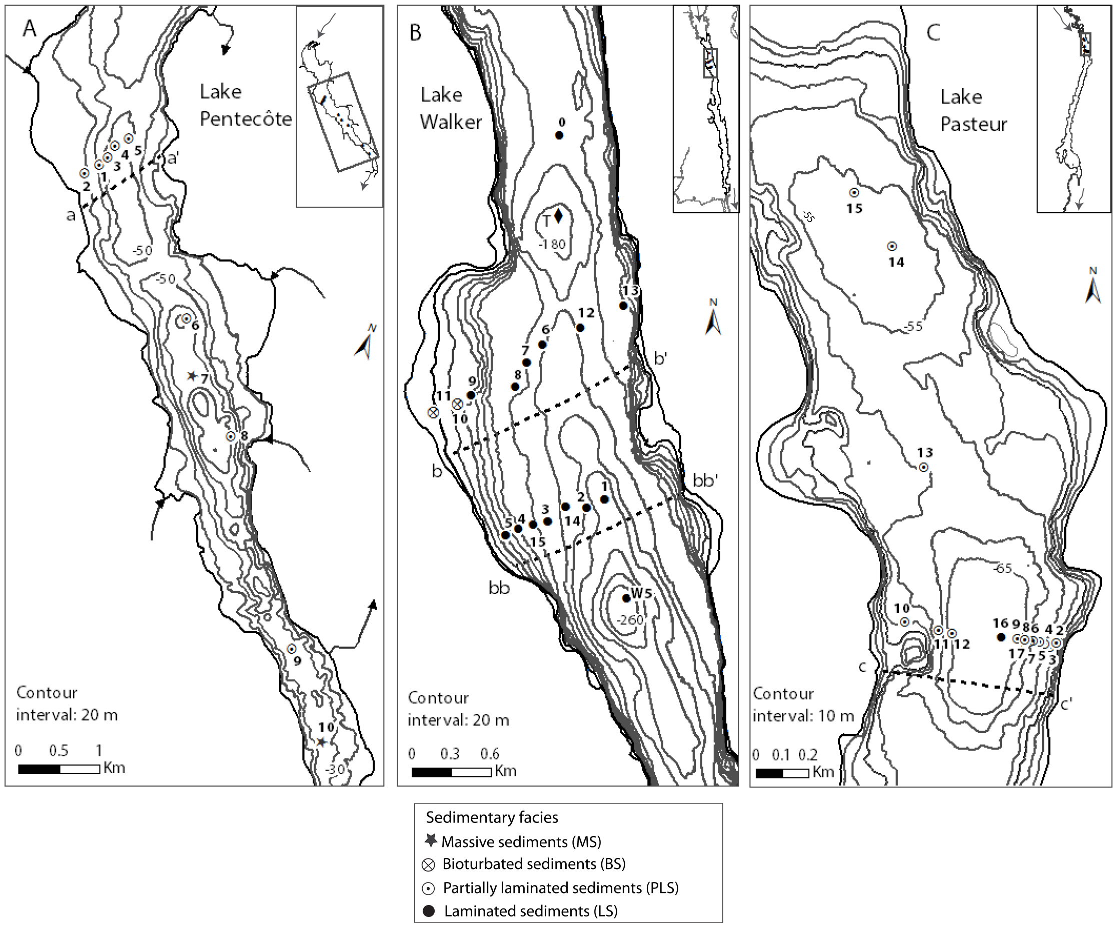

Fig. 2. Maps showing bathymetry, location of sediment cores and the sediment facies described in (A) Lake Pentecôte, (B) Lake Walker and (C) Lake Pasteur. Core names are abbreviated as serial numbers e.g. WA14-**06**-R written as 6 (Table 1). W5 refers to the reconnaissance core, WA11-**W5**-R from Lake Walker (see text). Also shown is the deployment location of Onset temperature sensors in Lake Walker, labelled as T. Schematic subbottom profiles along marked transects are shown in Fig. 3. Core names along transect c-c', Lake Pasteur, are clearer in Fig. 4D

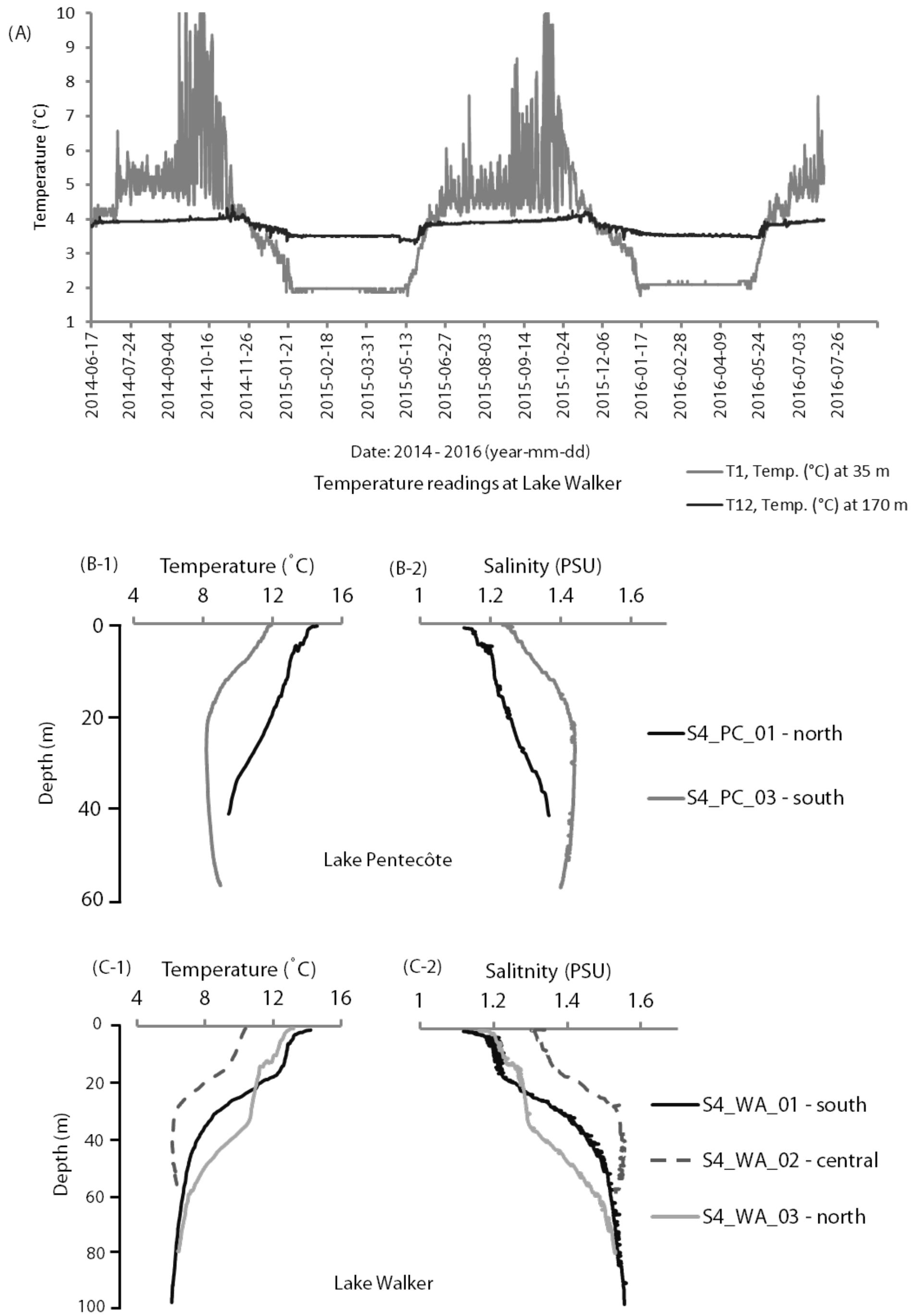

Fig 3. Measurement of physical parameters: (A) Temperature variations in the water column of Lake Walker at 35 and 170 m depths below water level measured using Onset Hobo temperature sensors over a 2-year period (June 2014 - August 2016). Deployment location of sensors is marked as T in the Fig. 2. (B and C) Profiles of temperature and salinity measured in lakes Pentecôte and Walker, respectively using an S4 current meter on September 24 2014 (sampling points are described in Table 3).

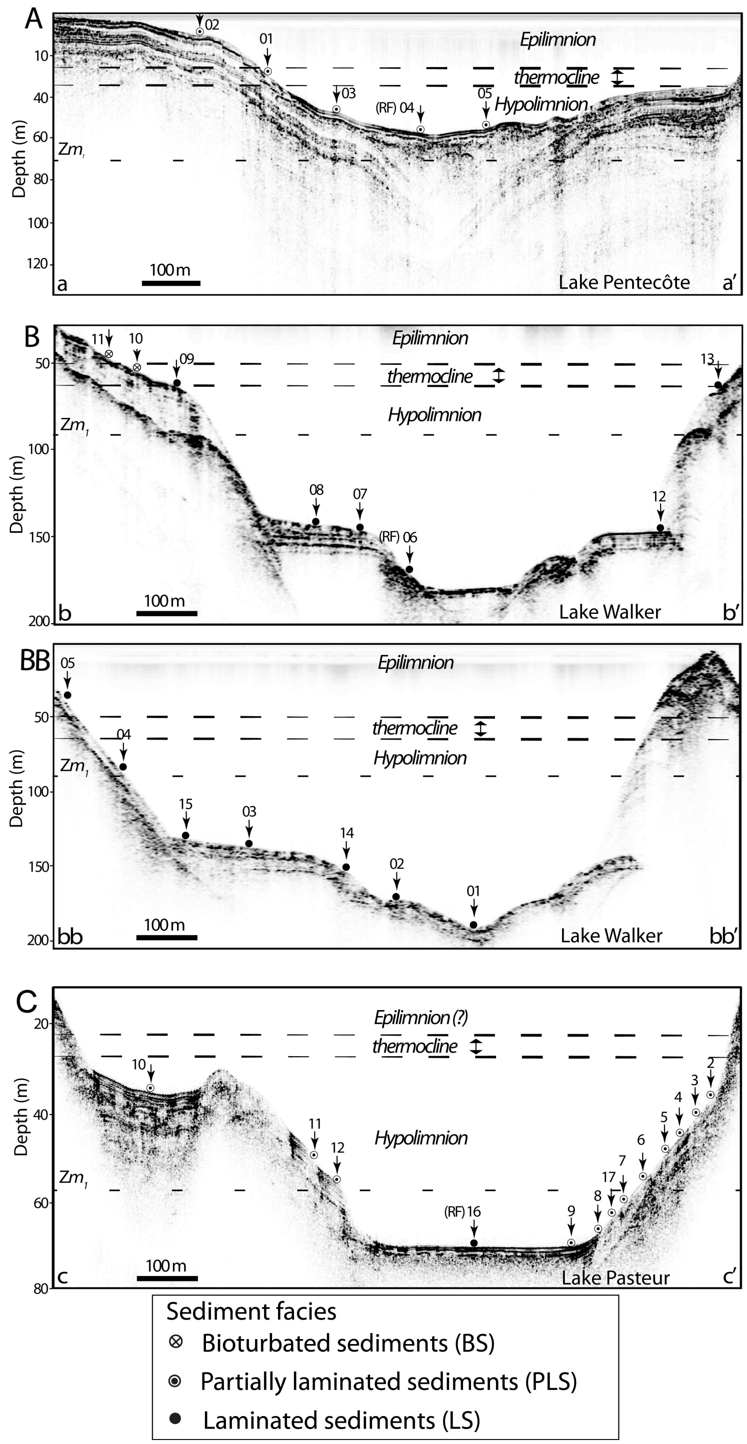

Fig. 4. Schematic subbottom profiles along the transects shown in Fig. 2. (A) a – a', Lake Pentecôte; (B) (b – b', bb – bb', Lake Walker) and (C) c – c', Lake Pasteur. The location of cores retrieved and the sediment facies encountered are shown (see full legend in Fig. 2). Core names are abbreviated as serial numbers (see Table 1). RF indicates the reference core for each lake. Thermal stratification zones are inferred from temperature measurements (see text). Also shown are the empirical depths of the critical boundary (Zm_1) described for each lake (See text and Table 1)

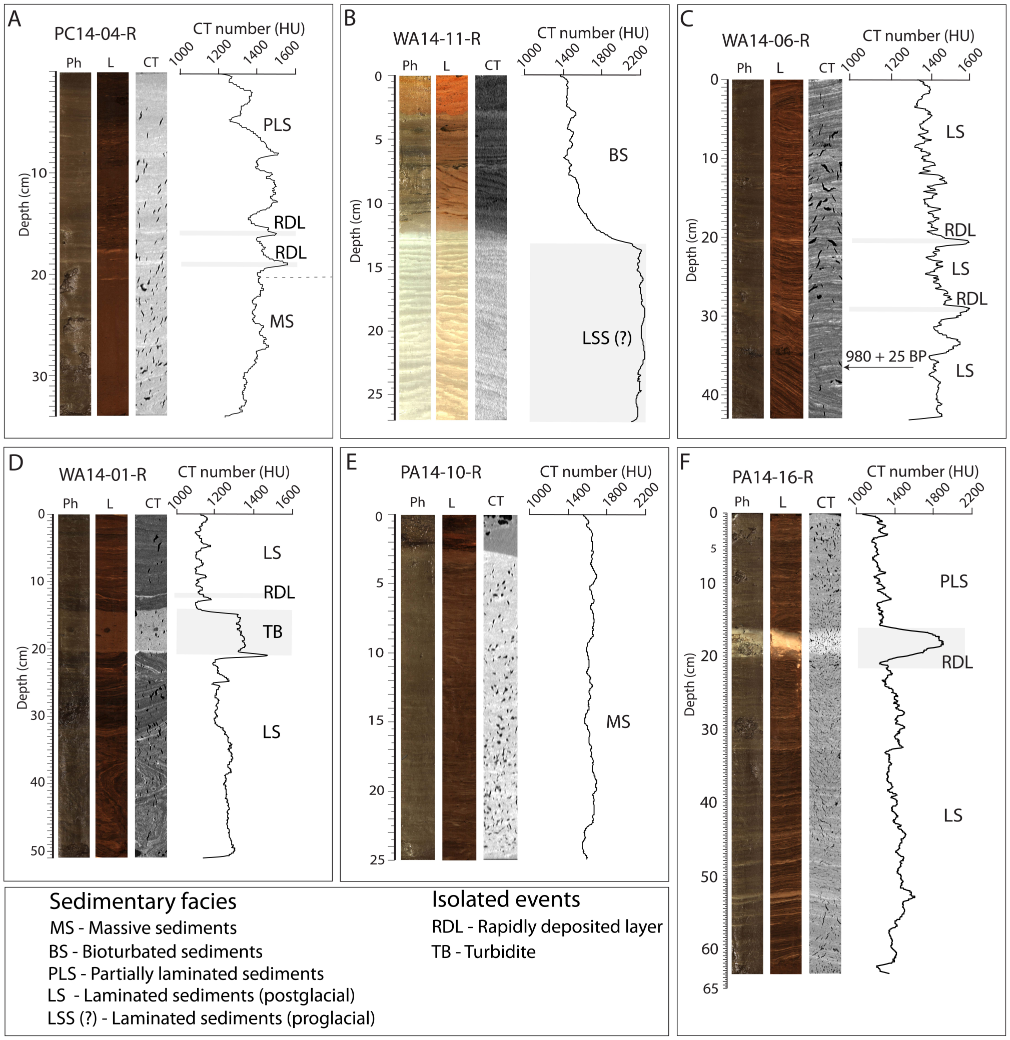

Fig. 5. Digital photo (Ph), ITRAX line scan images (L) and CT-scan frontal view (CT) showing example images of the sedimentary facies described in lakes Pentecôte, Walker and Pasteur. Rapidly deposited layers (RDLs) and turbidites (TB) represent isolated events. The LLS (?) represents proglacial facies that was encountered (below the BS facies, 5B) but not discussed in detail in this study (see G. Poiré et al. accepted). Note that corresponding images may appear slightly different because they were taken along different slices/views of the respective sediment cores

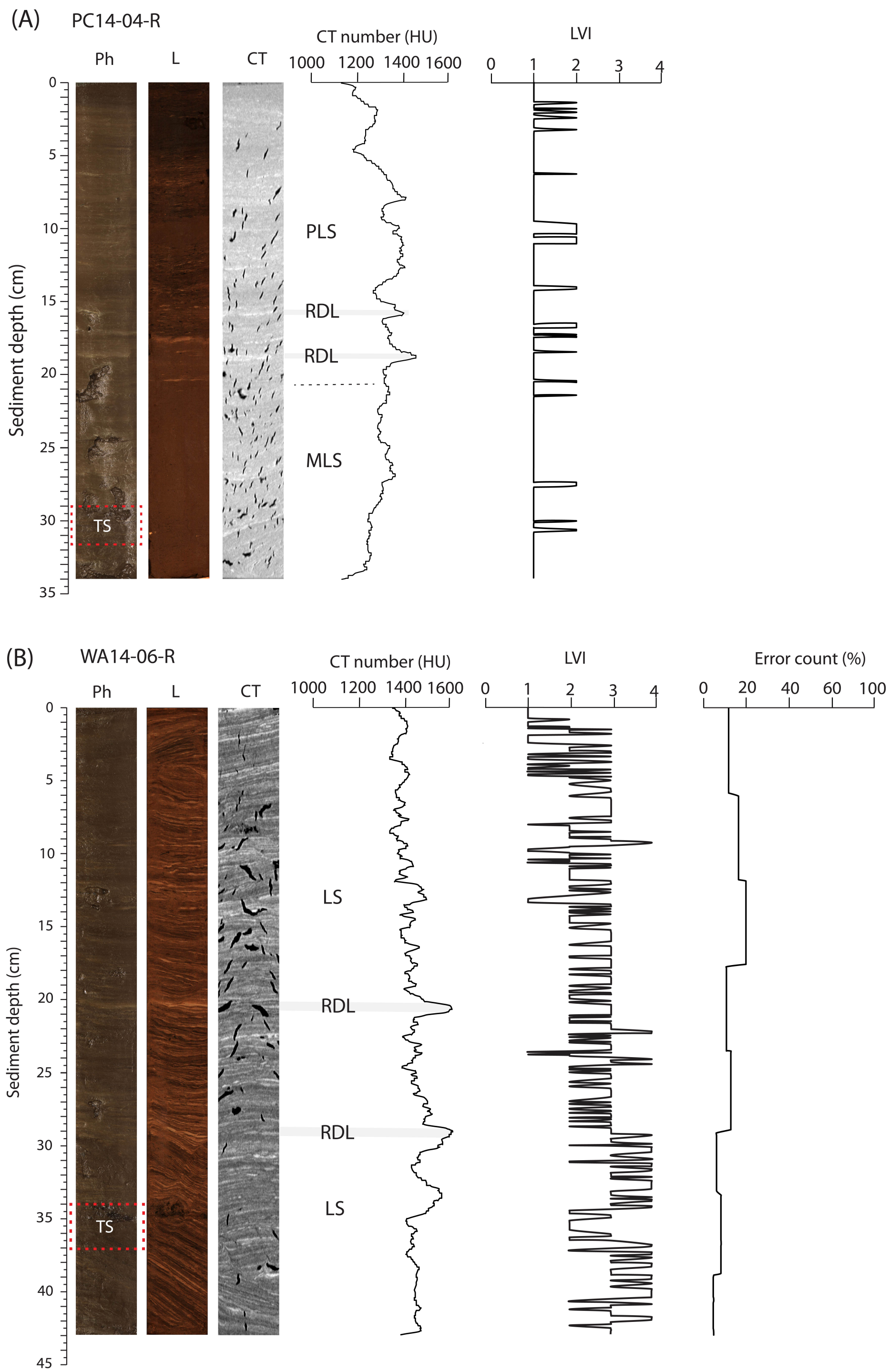

Fig. 6. Profiles with the digital photo (Ph), ITRAX line scan image (L) and CT-scan frontal view (CT), and results of sedimentological analysis: laminae visibility index (LVI) and laminae counting error estimate for the reference cores (A) PC14-04-R, (B) WA14-06-R and (C) PA14-16-R from lakes Pentecôte, Walker and Pasteur, respectively. LVI index: 0 - none, 1- faint, 2 - visible, 3 - clear, 4 - distinct. Thin-sections from the lower part (marked "TS" on the digital photos) are shown in Fig. 7.

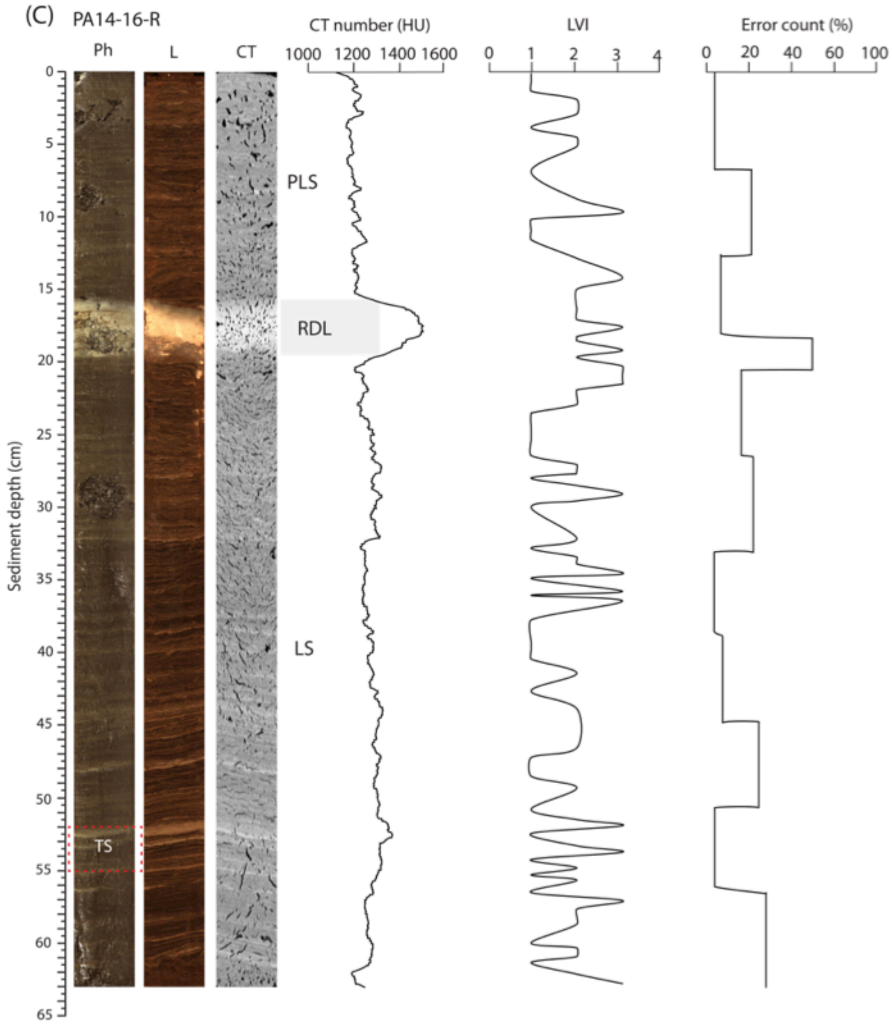

Fig. 6 (continued, 6C) Profiles with the digital photo, CT-scan frontal view, line scan image (ITRAX) and results of sedimentological analysis: laminae visibility index (LVI) and laminae counting error estimate for the core PA14-16-R from Lake Pasteur. LVI index: 0 - none, 1- faint, 2 - visible, 3 - clear, 4 - distinct. Thin-sections from the lower part (marked “TS” on the digital photos) are shown in Fig. 7.

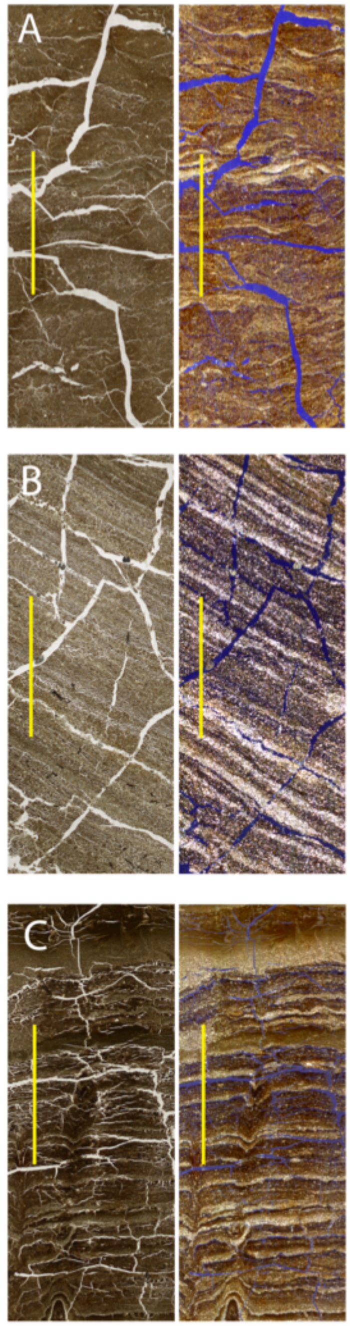

Fig. 7. Image observation of laminae structure in lower intervals of the reference cores: (A) PC14-04-R, (B) WA14-06-R and (C) PA14-16-R using thin-sections viewed in plane (left) and cross polarized light (right). Scale is 1 cm. Blue backgrounds in the cross-polars are due to the embedding resin. In the WA14-06-R and PA14-16-R, visible–distinct laminae couplets comprising a silty lamina and a clayey lamina with sharp contact with the overlying laminae can be seen

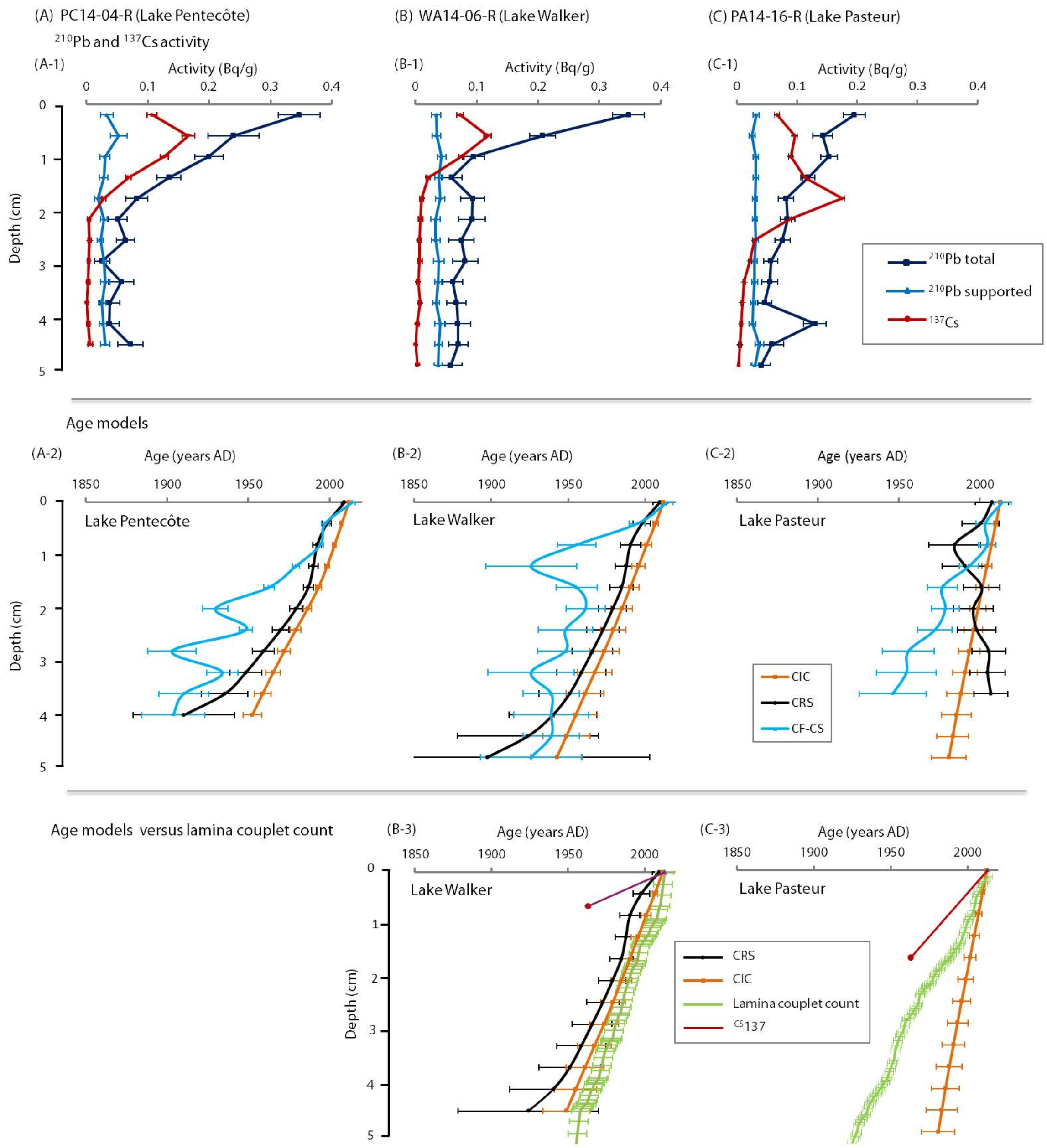

Fig. 8. Recent chronology (^{210}Pb and ^{137}Cs) for the reference cores from (A) Lake Pentecôte, (B) Lake Walker and (C) Lake Pasteur, respectively: (A-1, B-1, and C-1) Total (measured) and supported (from ^{226}Ra decay) ^{210}Pb activity and ^{137}CS activity; (A-2, B-2, and C-2) Chronology models based on the constant rate of supply (CRS), the constant initial concentration (CIC) and constant flux–constant sedimentation (CF-CS); (B-3, and C-3) Comparison of applicable age models (CIC/CRS) to lamina couplet counts in the upper sediments of lakes Walker and Pasteur